Continued development of the pulsed magnetic nozzle for the Pulsed Fission Fusion (PuFF) vehicle

Nathan M. Schilling* and Jason T. Cassibry.†
University of Alabama in Huntsville, Huntsville, AL, 35899, U.S.A

Robert B. Adams‡
National Aeronautics and Space Administration, George C. Marshall Space Flight Center, MSFC, AL 35812

High thrust, high specific impulse propulsion systems, such as PuFF (Pulsed Fission-Fusion) offer a new paradigm of speed and safety when exploring the solar system. To realize these possibilites, PuFF needs a mature magnetic nozzle design. PuFF's magnetic nozzle is unique in that it must provide power in addition to thrust. In the authors' opinion, the power system design is fairly mature, but nozzle thrust coil design is less so. Previous work has suggested that the PuFF magnetic nozzle will behave similarly to a 'magnetic reflection chamber,' relying on principles of magnetic flux compression to re-direct nozzle flow. However, recent work, using the 3D modeling software SPFMax, suggests that plasma motion in the nozzle will be driven by the Lorentz force. This recent work is limited in that the plasma did not completely leave the nozzle before the simulation ended. In this work, we aim to extend the SPFMax model from previous work, with a bolstered electromagnetic field solver, so the model can run until the plasma is fully evacuated. We hope to confirm previous results regarding the ideal PuFF nozzle design, but we could be surprised. Through improving the PuFF nozzle model, we aim to reduce technical risk with building the nozzle, realize paradigm-shifting performance numbers, and allow rapid, reliable, and safe exploration of the solar system.

I. Introduction

Current missions are hampered by long trip times. With current propulsion technology, crewed Mars missions take 1-2 years [1] and robotic sample return missions take in excess of 40 years [1]. These long trip times represent a significant hazard, especially for crewed Mars missions, where higher trip times can cause in increased radiation and micro-gravity damage to the crew. It has been know since at least the 1960s that nuclear fission, fusion, or hybrid-fission fusion systems can reduce these trip times by an order or magnitude [1]. Of the three, hybrid fission-fusion systems are attractive given their reduced technology development when compared to fusion systems, while offering higher specific impulse than pure fission systems. One system, the Pulsed Fission-Fusion (PuFF) spacecraft can reach Mars in a little over a month, Jupiter in a little over a year, and the interstellar precursor in a little over 35 years [2], making PuFF an attractive option for interplanetary propulsion.

PuFF works by storing energy in Linear Transformer Drivers (LTDs) that create a high-voltage high-current pulse (a Z-pinch pulse), and induce nuclear fission and fusion in a target [3]. The nuclear reactions create a large energy release that heats the target to a plasma state [3], which allows the target to be manipulated by magnetic fields. Accordingly, the magnetic nozzle interacts with the target, producing jet power, and producing some energy that goes back into the LTDs [4]. As the LTDs output a power pulse, PuFF is a pulsed vehicle, making the magnetic nozzle a pulsed magnetic nozzle. Pulsed nozzles have important physical differences from steady-state magnetic nozzles, instead of accelerating flow they need to reflect it. Accordingly, instead of the conventional de Laval nozzle shape, they appear parabolic or hemispherical [3–9]. Most PuFF vehicle subsystems are fairly mature [2, 3, 10]; the details of the lithium injection system have been mostly determined [3], trade studies on the radiation shield have been performed [3], the heat rejection system has been sized [3]. Additionally, within the magnetic nozzle subsystem, the power generation subsystem is well developed [9–11]. Magnetic flux compression, the physical process that underpins the power generation system, is fairly well understood,

*Graduate Research Assistant, Department of Mechanical and Aerospace Engineering, 301 Sparkman Dr NW, Huntsville, AL 35899, AIAA Student Member.
†Associate Professor, Department of Mechanical and Aerospace Engineering, 301 Sparkman Dr NW, Huntsville, AL 35899, AIAA Associate Fellow.
‡Advanced Propulsion Engineer, Propulsion Research and Technology Branch, MSFC, AL 35812, AIAA Associate Fellow.

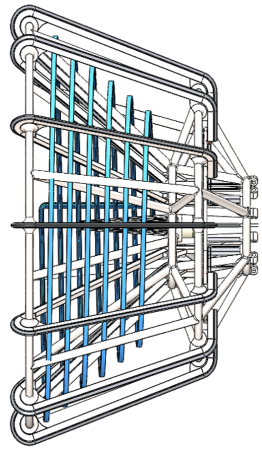

Fig. 1 Image of the current PuFF magnetic nozzle. ***Image credit Augustin Demonceaux. Nozzle thrust coils in black and white, power generation system in blue.***

with a fair amount of physical modeling done, and several designs put forward [10, 11]. However, the physical processes that underpin the nozzle are not as well understood; leaders in the field thought that magnetic flux compression also underpins nozzle design, but recent work suggests this isn't the case [12]. Instead, the Lorentz ($\boldsymbol{j} \times \boldsymbol{B}$) force dominates, leading to a magnetic nozzle design that looks different from previous work. However, the authors of Ref. [12] leave confirmation of their novel conclusions to future work. Additionally, in Ref. [12] the plasma doesn't fully expand (as the simulation crashes before the plasma can expand), leaving developing a model that can fully expand to future work.

In this work, we aim to address the future work of Ref. [12]; we aim to leverage the model developed in Ref. [12] to simulate a plasma expanding in a magnetic nozzle. We also aim to confirm (or refute) the conclusions that Cassibry, Schillo, and Winterling draw.

II. Background

A magnetic nozzle is a device in a propulsion system that takes high-enthalpy plasma and uses magnetic fields to produce thrust/impulse bit and specific impulse. A magnetic nozzle is different from a conventional metal nozzle in that a magnetic nozzle interacts with the plasma electromagnetically, rather than via contact. The magnetic nozzle considered for PuFF is different from other magnetic nozzles in that it is pulsed, meaning propellant was injected, would expand, and then would completely evacuate the nozzle before the next propellant injection; propellant was not constantly injected into the nozzle.

A pulsed magnetic nozzle is shown in operation in Fig. 2. In Fig. 2a, the nozzle is shown in it's initial state, with the plasma inside the nozzle, and with the magnetic field from the nozzle fully filling the nozzle. As the plasma is hot, it expands, and because it is electrically and magnetically conductive, it generates it's own internal magnetic field to exclude the applied magnetic field from the nozzle [13], shown in Fig. 2b. This process continues until the plasma expands to it's fullest. As the plasma expands, it compresses the applied magnetic field, increasing the strength of the field, and making the field push on the plasma harder, until the field stops further expansion of the plasma. At this stage, the plasma transfers some of its momentum to the nozzle, giving thrust generation (green arrows in Fig. 2b). Afterward, the magnetic field continues to push on the plasma, pushing it away from the nozzle and out the back of the vehicle (Fig. 2d), increasing thrust output by the nozzle.

A. Previous work and the magnetic reaction chamber

The first known concept employing a magnetic nozzle the authors could find is Daedalus [14]. Daedalus is a two-stage laser-fusion propulsion system. It creates high-enthalpy exhaust using an Inertial Confinement Fusion (ICF) reactor. The exit temperatures from the reactor are so hot conventional metal-walled nozzles would melt; hence the use of a magnetic nozzle. However, due to the ICF nature of the reactor, the reactor was operated in a pulsed mode. First, propellant would be injected into the reactor. Next, the laser guns were turned on, initiating fusion in the propellant. The propellant, now hot enough to be a plasma, would be pushed out the back of the vehicle by the magnetic nozzle.

Table 1 Magnetic nozzle input conditions for Ref. [7] and Ref. [8]

Parameter	Plasma-gun (Ref. [7])	Z-pinch (Ref. [8])
m_0 (kg)	0.002	0.02
E_{th_0} (MJ)	906	584
d (m)	2	2
R_{p_0} (m)	0.3	0.3

Then, propellant would be re-injected into the reactor and the cycle would start again. Because the reactor was located inside the magnetic nozzle, the magnetic nozzle was called a "magnetic reaction chamber" - a name that stuck in some subsequent literature [5].

Ref. [5] has a similar design to Daedalus, but uses particle beams instead of laser beams. Also, Winterburg's magnetic reaction chamber is "a concave magnetic mirror produced by superconducting field coils," which is slightly different from the Daedalus concept. Also, Winterberg correctly asserts that the "magnetic pressure of the field reflects the fireball generated by the explosion [the nuclear explosion]" [5]. This indicates that the magnetic pressure must be higher than the gasdynamic pressure for the magnetic nozzle to work. An offshoot of this concept is that the magnetic energy in the nozzle has to meet or exceed the thermal energy in the plasma to make the plasma deflect.

The next group uses this latter property in their investigation of investigate magnetic nozzle designs. The authors of Ref. [7, 8] design magnetic nozzles for pulsed fusion vehicles, similar to Ref. [5, 14]. However, instead of an ICF plasma source, they use a Magnetized Target Fusion (MTF) plasma source. In Ref. [7], the MTF reactor consists of a set of plasma guns, whereas in [8] the MTF reactor is a Z-pinch plasma source. The input conditions for both plasma sources are shown in Table 1. The plasma initial mass is m_0, the plasma initial thermal energy is E_{th_0}, the nozzle focus (where the plasma starts out relative to the bottom of the nozzle) is d, and the initial radius of the plasma is R_{p_0}. distance between Most notably, the plasma gun source has lower mass and higher thermal energy than the Z-pinch source.

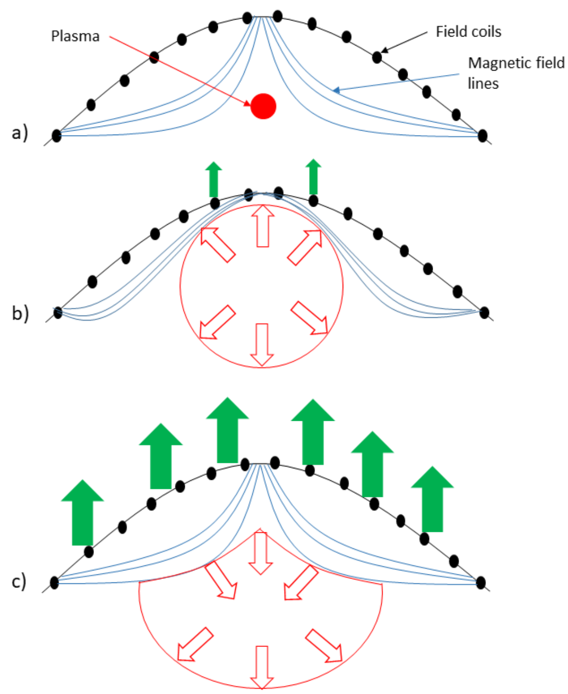

Fig. 2 Pulsed magnetic nozzle schematic. ***Thrust is represented by green arrows and plasma momentum by red arrows. Inspired by Fig. 1 in Ref. [6]***

Regardless of input condition, both plasmas are situated inside a magnetic nozzle (which isn't called a 'magnetic reaction chamber' even though it's the same as the device in Ref. [5, 14]). Both references use the same method to analyze plasma behavior inside the nozzle, where they spherically divide the plasma into several segments, and assume each segment spectrally reflects off a section of a parabolic magnetic field profile. This method does not consider the electrodynamic nature of the plasma, but acts as a good first-pass. Using this method, the authors of Ref. [7, 8] find an internal nozzle efficiency of 0.81 and 0.6 for the plasma guns concept [15] and the Z-pinch concept [8] respectively. Internal nozzle efficiency is defined according to Eq. (1)

$$\eta_{th} = \frac{m v_z}{E_{th_0}} \tag{1}$$

In Ref. [6], Romanelli et al. again return to the term "magnetic reaction chamber". They also consider the electrodynamic nature of the plasma using a 2D cylindrical ideal Magnetohydrodynamic (MHD) code called PLUTO. Ideal MHD codes do not consider resistive losses in the plasma, and both plasmas can be reasonably approximated

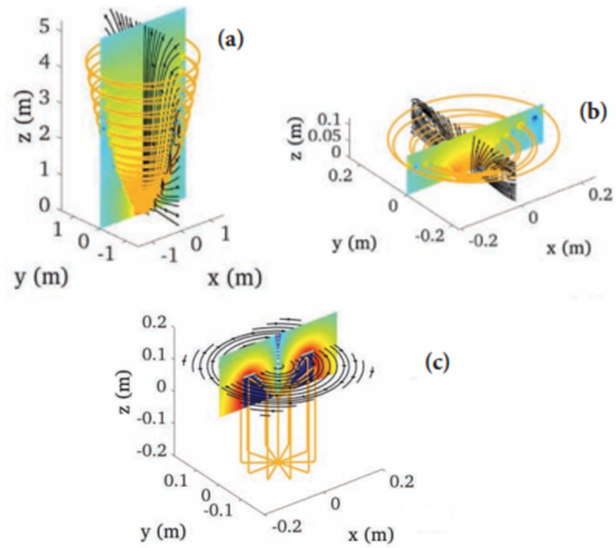

Fig. 3 Nozzle configurations considered in Ref. [12]. a) Solenoidal configuration, b) Trumpet configuration, c) Axial configuration *Adaptation of Figs. 2-3 in Ref. [12]*

using ideal MHD theory [6]. Romanelli et al. analyze similar nozzles as the ones in Ref. [7, 8], taking the same plasma input conditions for both. They use the same 8-turn solenoid for both, with the same coil radial positions, but different currents going through each nozzle. Since the plasma-gun input condition has higher energy, it's nozzle has higher currents than the Z-pinch plasma, to match the energy of the plasma to the energy of the nozzle [5]. Taking this difference into account, and running the nozzles through PLUTO until the plasma completely left the nozzle (14-42 μ s), Romanelli et al. found the internal nozzle efficiency for both concepts to be around 0.6, which is slightly lower than the authors of Ref. [7, 8] got using their lower-fidelity model. Romanelli et al. suggest their results could be expended by analyzing the same magnetic nozzles with higher fidelity codes - specifically ones that are non-ideal (resisitve) and 3D.

B. Alternate theories - Lorentz force acceleration

One such non-ideal 3D MHD code is the Smoothed Particle Fluid with- Maxwell, or SPFMax, equation solver. In Ref. [12]. Cassibry, Schillo, and Winterling use SPFMax to analyze 3 different magnetic nozzle configurations; a solenoidal configuration, a trumpet configuration, and a axial configuration, all shown in Fig. 3.

Each configuration is selected to give a magnetic field with a different topology; the solenoidal configuration gives a primarily axial magnetic field topology, the trumpet configuration gives a primarily radial topology, and the axial configuration gives a primarily azimuthal topology. Cassibry, Schillio, and Winterling use different plasma input conditions from prior work; they consider a Deutrium-Tritium plasma with "an initial density of 80 kg/m^3 and a temperature of 1 keV. The target was 1 mm in radius, 1 cm in length, and has a mass of 2.5 mg". This is a much lower mass, lower initial energy (0.2 MJ vs. 584-906 MJ) target than Ref. [6–8].

Leveraging SPFMax, Cassibry, Schillio, and Winterling find that the axial configuration (Fig. 3c) gives the highest performance; when augmented with a pusher plate it gives a nozzle efficiency of 0.2. Note that this is less than the efficiencies of [6–8], but this is because of target properties and SPFMax considering radiative cooling. The target in Ref. [12] is lower mass and lower energy than Ref. [7, 8], so there is less energy available for performance, and accordingly the results of Ref. [12] show less performance. Also, Ref. [12] considers radiative cooling of the plasma, reducing energy available for performance even further. Ref. [12] finds a specific impulse of 9000 sec, which is higher than the 5000 sec with just the pusher plate, showing the magnetic nozzle offers and improvement over a pure pusher plate. However, the specific impulse is less than that found in Ref. [6] (61000 sec, 19000 sec), but this is also probably because aforementioned reasons.

Cassobry, Schillo, and Winterling primarily identify simulation time as an area for future work; they are only able to run their case of 0.25 μ s rather than the 14-42 μ s from Ref. [6]. It is unclear whether the plasma fully leaves the nozzle after 0.25 μ s - meaning there is still performance left in the plasma. So, the efficiency in Ref. [12] might be low because the simulation hasn't run it's full course and the plasma hasn't fully expanded. The simulation stops at 0.25 μ

s because the simulation crashes due to oscillations in the electric and magnetic field. These oscillations need to be addressed in future work, potentially by a current dampening term. Then, the simulation can be run to completion.

III. Methodology

For this work, we use a modified version of SPFMax to analyze our magnetic nozzles. We used SPFMax because it is a fully-3D code, and because it is able to compute problems involving complex plasma and magnetic nozzle geometries fairly quickly. It does not offer the same fidelity as Particle-In-Cell (PIC) codes [13] but it is faster, and can be run on a desktop machine.

A. SPFMax

Of primary importance in SPFMax is the fluid model, which uses Smooth Particle Hydrodynamics (SPH). SPH uses a kernel function to approximate properties in the following manner:

$$A_a(r) = \int A(r')W(r - r', h)dr' \tag{2}$$

A is any property (such as pressure, temperature, etc), subscript a indicates point a, r is the position of point a in space, h is the compact support distance and W is the interpolating kernel function [16]. The integral is then replaced with a summation over b neighboring particles as follows

$$A_a = \sum_b A_b V_b W_{ab} r - r', h) \tag{3}$$

with V_b being the volume of neighboring b number of particles [16]. W_{ab} is the cubic-spline function, which is as follows

$$W_{ab}(q) = \begin{cases} \frac{1}{4\pi h_{ab}^3}[(2-q)^3 - 4(1-q)^3] & \text{for } 0 \le q \le 1 \\ \frac{1}{4\pi h_{ab}^3}(2-q)^3 & \text{for } 1 \le q \le 2 \\ 0 & \text{for } q \ge 2 \end{cases} \tag{4}$$

where h_{ab} is again the compact support distance, which must be chosen according to the following equations

$$\sum_b V_b W_{ab} = 1 \tag{5}$$

equations

$$\sum_b V_b \nabla W_{ab} = 0 \tag{6}$$

where ∇W_{ab} denotes the gradient of the kernel function [16]. Choosing h is the most important, but also most difficult part of the model [16]. In implementation, the SPFMax code considers b=60 (60 nearest neighbors), and for a full expansion of h, see Ref. [16]. The equations of motion the code solves are the continuity, momentum, and energy equations:

$$\frac{\partial \rho}{\partial t} + \nabla \cdot (\rho \vec{u}) = 0 \tag{7}$$

$$\frac{\partial \vec{u}}{\partial t} = -\frac{1}{\rho}\nabla p + \nabla \cdot \tau + \frac{1}{\rho}(\vec{j} \times \vec{B}) = 0 \tag{8}$$

$$\frac{\partial e}{\partial t} = -\frac{p}{\rho}\nabla \cdot \vec{u} + \frac{1}{\rho}\tau : \nabla \vec{u} - \nabla \cdot (k\nabla T) - 4\sigma_{sb}T^4\chi_{Planck} + \frac{\eta}{\rho}j^2 \tag{9}$$

where ρ is the mass density, $\vec{u}$ is the velocity vector, $\vec{j}$ is the current density vector, $\vec{B}$ is the magnetic field, t is time, p is the static pressure, τ is the deviatoric viscous stress tensor, k is the thermal conductivity, σ_{sb} is the Stefan-Boltzmann constant, T is temperature, χ_{Planck} is the single group Planck emission opacity, and η in these equation is a parameter set by SPH theory to be 1.11 [16].

In Ref. [12] Maxwell's equations are formulated in terms of the electric field scalar potential and magnetic vector potential, but in this work we use the magnetic field rather than the magnetic vector potential. This is because it is easier to set/calculate the magnetic field at the nozzle computational boundary rather than the magnetic vector potential. While there is functionality for it, we do not use the electric potential, as we do not electrically connect the plasma to our device. Electric and magnetic fields are propagated through the plasma using "a network of transmission lines integrating Kirchoff's voltage and current laws in which additional physics include back electromotive force (EMF), and the Hall Effect as needed. Field propagation is accomplished by utilizing a superposition of current sources using Biot Savart's law. " [12]. Currents are found using Ohm's law (Eq. (10).

$$\vec{j} = j_{scale}\sigma(\vec{E} + \vec{u} \times \vec{B}) \tag{10}$$

Here, the plasma conductivity is σ, and j_{scale} is a scalar that ensures the current density doesn't change too quickly. This reduces the electromagnetic oscillations from the version of SPFMax in Ref. [12], and will hopefully allow our version of the code to run past 0.25 μ s.

To integrate the equations of motion, we use the 2nd order Runge-Kutta scheme.

We compiled SPFMax on a Windows 10 Enterprise machine with an Intel(R)Xenon(R) E5-1630 v4 CPU running at 3.70 GHz, and an NVIDA Quatro M5000 graphics card. SPFMax is implemented in MATLAB with the GPU computing toolbox [17].

B. Study design

For our study we again used internal nozzle efficiency (see Eq. (1)) as our figure of merit. For our plasma, we considered a 0.6 kg plasma which is 0.1 kg of Uranium simulant (Tungsten) and 0.5 kg of lithium, with the Uranium stimulant at 1 keV and the lithium at room temperature. We considered an axial nozzle with 16 struts, and a solenoid with 16 turns. The Tungsten starts 1 m away from the start of both nozzles. Both nozzles carry coil currents of 10 MA.

IV. Results

A. Current progress

Runs in SPFMax were done with a 1 keV plasma expanding into a axially-wound nozzle topology (Fig. 3 in Ref. [12]) with 16 struts, each strut having a coil current of 1 MA. Specific impulse and nozzle efficiency are plotted below. As shown in Fig. 4-5, the plasma begins to expand regularly and linearly, until a little over 1 μ s into the simulation, wherein it begins to behave non-linearly. This non-linearity results in the solver diverging, giving negative specific impulse and efficiencies drastically bigger than 1, which are both non-physical effects. So far, the model has improved on previous work and was able to run to about 1100 ns. This represents a 4x improvement over Ref. [12]. However, the plasma still isn't able to fully leave the nozzle. We aim to fix this before publication.

V. Conclusion

In conclusion, for advanced nuclear propulsion system like PuFF, the highest-performing nozzle is (probably) the axial-wound one. It generates high thrust, and fairly high specific impulse. These performance numbers emphasize the potential of advanced nuclear propulsion systems, allowing for safer crewed Mars missions, and opening up sample return missions to the outer planets. This work reduces the technical risk of such systems, and with a complementary experimental program to bolster these findings, could realize the potential of advanced nuclear propulsion.

Acknowledgments

This research was supported by a NASA Space Technology Research Fellowship.

References

[1] Cassibry, J. T., Cortez, R., Stanic, M., Watts, A., Seidler, W., Adams, R. B., Statham, G., and Fabisinski, L., "Case and Development Path for Fusion Propulsion," *Journal of Spacecraft and Rockets*, Vol. 52, No. 2, 2015, pp. 595, 612. https://doi.org/10.2514/1.A32782.

[2] Cassibry, J., Bradley, D., Fabisinski, L., Statham, G., and Adams, R., "Developing the Pulsed Fission-Fusion (PuFF) Engine," *50th AIAA/ASME/SAE/ASEE Joint Propulsion Conference AIAA*, AIAA, Cleveland, OH, US, 2014, pp. 1–14. URL https://ntrs.nasa.gov/search.jsp?R=20140012884.

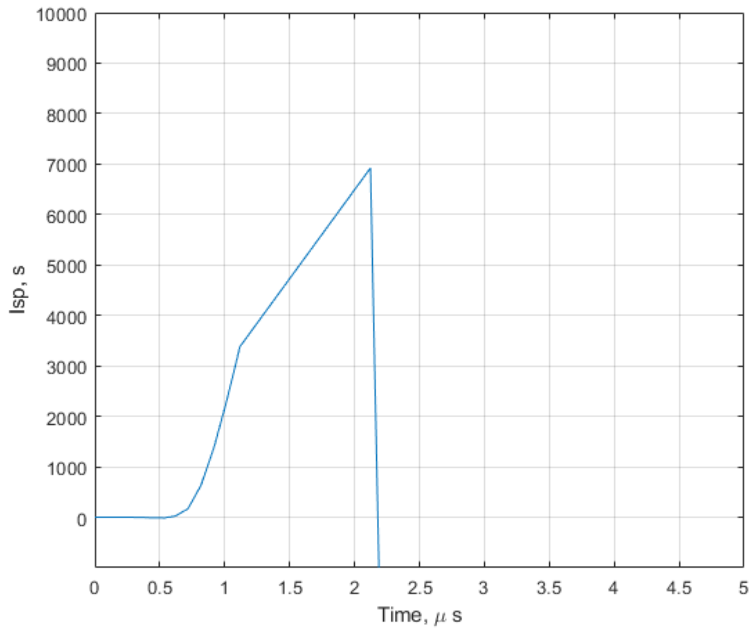

Fig. 4 Specific impulse for a 1 keV plasma in a 16 strut magnetic nozzle, each strut having a coil current of 1 MA.

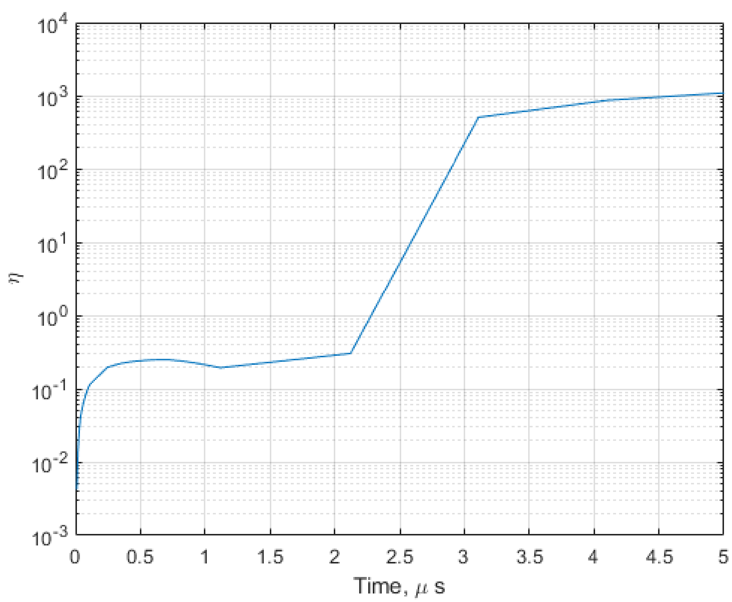

Fig. 5 Nozzle for a 1 keV plasma in a 16 strut magnetic nozzle, each strut having a coil current of 1 MA.

[3] Adams, R. B., Cassibry, J. T., Schillo, K. J., and Taylor, B. D., "The Pulsed Fission-Fusion (PuFF) Engine-Nacelle Concept and Development Roadmap," *ASCEND 2020*, AIAA, Virtual event, 2020, p. 4082. URL https://arc.aiaa.org/doi/abs/10.2514/6.2020-4082.

[4] Adams, R., Cassibry, J., Bradley, D., Fabisinski, L., and Statham, G., "Pulsed Fission-Fusion (PuFF)–Phase I Report," *NASA Innovative and Advanced Concepts Final Report*, 2013.

[5] Winterberg, F., "Rocket propulsion by thermonuclear micro-bombs ignited with intense relativistic electron beams." 1971.

[6] Romanelli, G., Mignone, A., and Cervone, A., "Pulsed fusion space propulsion: Computational Magneto-Hydro Dynamics of a multi-coil parabolic reaction chamber," *Acta Astronautica*, Vol. 139, 2017, pp. 528–544.

[7] Adams, R., Alexander, R., Chapman, J., Fincher, S., Hopkins, R., Philips, A., Polsgrove, T., Litchford, R., Patton, B., Statham, G., White, P., and Thio, F., "Conceptual Design of In-Space Vehicles for Human Exploration of the Outer Planets," Tech. Rep. NASA/TP—2003–212691, National Aeronautics and Space Administration, November 2003.

[8] Polsgrove, T., Adams, R. B., Fabisinski, L., Fincher, S., Maples, C. D., Miernik, J., Percy, T., Statham, G., Turner, M., Jason Cassibry, J., Cortez, R., and Santaruis, J., "Z-pinch pulsed plasma propulsion technology development," Tech. Rep. 20110008519, National Aeronautics and Space Administration, Oct 2010.

[9] Schilling, N., Cassibry, J., and Adams, R., "Development of a pulse-recharge magnetic nozzle for PuFF," *AIAA Propulsion and Energy 2019 Forum*, AIAA, Indianapolis, IN, US, 2019, pp. 1–18. https://doi.org/10.2514/6.2019-4284, URL https://arc.aiaa.org/doi/abs/10.2514/6.2019-4284.

[10] Schilling, N., Cassibry, J. T., and Adams, R. B., "Elements of an Inductive Electrical Power Conversion System for Fusion-Class Plasmas," *AIAA Propulsion and Energy 2020 Forum*, 2020, p. 3539.

[11] Schilling, N., Cassibry, J., and Adams, R., "Developing a charging subsystem for the PuFF engine," *70th International Astronautical Congress*, International Astronautical Federation, 100 Avenue de Suffren, Paris, France, 2020, p. 123. https://doi.org/IAC-20-C4-10-C3.5-1-x56672.

[12] Cassibry, J., Schillo, K., and Winterling, B., "Pulsed Magnetic Nozzle for Fusion Propulsion," *Journal of the British Interplanetary Society*, Vol. 71, 2018, pp. 119–125.

[13] Morita, T., Edamoto, M., Miura, S., Sunahara, A., Saito, N., Itadani, Y., Kojima, T., Mori, Y., Johzaki, T., Kajimura, Y., et al., "Control of unsteady laser-produced plasma-flow with a multiple-coil magnetic nozzle," *Scientific reports*, Vol. 7, No. 1, 2017, pp. 1–7. https://doi.org/10.1038/s41598-017-09273-3.

[14] Bond, A., and Martin, A., "The Propulsion System, Parts 1 and 2," *Project Daedalus: the Final Report on the BIS Starship Study, ed. AR Martin, supplement to JBIS*, 1978, pp. 44–82.

[15] Thio, Y., Freeze, R., Kirkpatrick, R., Landrum, B., Gerrish, H., and Schmidt, G., "High-Energy Space Propulsion based on Magnetized Target Fusion," *35th Joint Propulsion Conference and Exhibit*, AIAA-99-2703, Los Angeles, CA, 1999. https://doi.org/10.2514/6.1999-2703.

[16] Cassibry, J. T., Cortez, R., Cody, C., Thompson, S., and Jackson, L., "Three dimensional modeling of pulsed fusion for propulsion and terrestrial power using smooth particle fluid with Maxwell equation solver (SPFMaX)," *53rd AIAA/SAE/ASEE Joint Propulsion Conference*, 2017, p. 4677.

[17] Shampine, L. F., and Reichelt, M. W., "The MATLAB ODE Suite," *SIAM Journal on Scientific Computing*, Vol. 18, 1997, p. 1–22. https://doi.org/10.1137/S1064827594276424.